

Chaos in Cross-Coupled BVP Oscillators

Tetsushi Ueta* and Hiroshi Kawakami†

September 14, 2004

Abstract

In this letter, we investigate the cross-coupled BVP oscillators. A single BVP oscillator has two terminals which can extract an independent state variable, so in the preceding works, several coupling systems have studied. Synchronization modes and chaos in these systems are classified as results of bifurcation problems. We revisit one of coupled oscillator, and clarified new results which have not been reported before, i.e., stable tori and its breakdown, and chaotic motions. Also classification of synchronized periodic solutions is done by a bifurcation diagram.

Keywords: BVP oscillator, bifurcation, torus doubling, chaos

1 Introduction

The BVP (Bonhöffer van der Pol) equation has been derived as a simplified model of Hodgkin-Huxley (abbr. HH) equation by FitzHugh and Nagumo. They reduced the HH equation (four-dimensional) to a two-dimensional system called the BVP equation or FitzHugh-Nagumo model by extracting excitability of the dynamics of the dynamic behavior in the HH equation. The BVP oscillator has two terminals which can extract two independent variables, v and i .

Papy et al., [Papy & Kawakami, 1995, Papy & Kawakami, 1996, Kitajima *et al.*, 1998] studied bifurcation structures and classification of synchronization phenomena in the resistively coupled BVP oscillators such as v - v , v - i couplings. They focused only on the behavior of the coupled system consisting of ‘identical’ oscillators, i.e., all oscillators have same parameter values and they are connected by same value of resistors. Group theory can help solving bifurcation problems of dynamical behavior and topological property of the specific symmetry system. Papy show many bifurcation diagrams of synchronized periodic solutions and their explanations by using group theory.

In this letter, we revisit the cross-coupled BVP oscillators (a special case of hybridly coupled oscillators[Papy & Kawakami, 1995] with $n = 2$), and show some new results. Firstly we formulate the system and indicate symmetrical properties of the equation. Secondly we show a bifurcation diagram of synchronized solutions in the parameter plane according to coupling coefficients. In-phase and anti-phase periodic solutions are classified by the tangent and Neimark-Sacker bifurcation curves. We also show a torus breakdown phenomenon

*Center for Advanced Information Technology, Tokushima University, Tokushima, 770-8506 Japan

†Faculty of Engineering, Tokushima University, Tokushima, 770-8506 Japan

which looks like the swollen shape type bifurcation[Sekikawa *et al.*, 2001] in four dimensional autonomous system. Finally we demonstrate a double scroll attractor via period-doubling bifurcation. The laboratory experiment results are shown.

2 Cross-coupled BVP oscillators

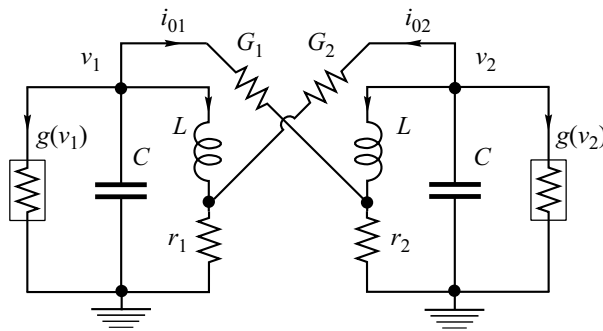


Figure 1: Asymmetrical Coupled BVP Oscillators

Figure 1 shows an asymmetrically coupled BVP oscillators. Coils and capacitors in both oscillators are identical. Then we have the following circuit equations:

$$\begin{aligned}
 C \frac{dv_1}{dt} &= -i_1 - g(v_1) - i_{01} \\
 L \frac{di_1}{dt} &= v_1 - r_1(i_1 + i_{02}) \\
 C \frac{dv_2}{dt} &= -i_2 - g(v_2) - i_{02} \\
 L \frac{di_2}{dt} &= v_2 - r_2(i_2 + i_{01})
 \end{aligned} \tag{1}$$

The currents of the coupling resistors are:

$$\begin{aligned}
 i_{01} &= G_1(v_1 - r_2(i_2 + i_{01})) \\
 i_{02} &= G_2(v_2 - r_1(i_1 + i_{02})).
 \end{aligned} \tag{2}$$

Solve Eq. (2) for i_{01} , and i_{02} , then by substituting them into Eq. (1), we have

$$\begin{aligned}
 C \frac{dv_1}{dt} &= -i_1 - g(v_1) - \frac{G_1}{1 + G_1 r_2}(v_1 - r_2 i_2) \\
 L \frac{di_1}{dt} &= v_1 - r_1 i_1 - \frac{G_2 r_1}{1 + G_2 r_1}(v_2 - r_1 i_1) \\
 C \frac{dv_2}{dt} &= -i_2 - g(v_2) - \frac{G_2}{1 + G_2 r_1}(v_2 - r_1 i_1) \\
 L \frac{di_2}{dt} &= v_2 - r_2 i_2 - \frac{G_1 r_2}{1 + G_1 r_2}(v_1 - r_2 i_2)
 \end{aligned} \tag{3}$$

The nonlinear negative conductance is modeled by

$$g(v) = -a \tanh bv.$$

Now we choose the following transformations:

$$\begin{aligned}x_j &= \frac{v_j}{a} \sqrt{\frac{C}{L}}, & y_j &= \frac{i_j}{a}, & k_j &= r_j \sqrt{\frac{C}{L}}, \\ \delta_j &= G_j \sqrt{\frac{L}{C}}, & j &= 1, 2. \\ \tau &= \frac{1}{\sqrt{LC}} t, & \gamma &= ab \sqrt{\frac{L}{C}},\end{aligned}$$

hence we have normalized differential equations as follows:

$$\begin{aligned}\dot{x}_1 &= -y_1 + \tanh \gamma x_1 - \frac{\delta_1}{1 + \delta_1 k_2} (x_1 - k_2 y_2) \\ \dot{y}_1 &= x_1 - k_1 y_1 - \frac{\delta_2 k_1}{1 + \delta_2 k_1} (x_2 - k_1 y_1) \\ \dot{x}_2 &= -y_2 + \tanh \gamma x_2 - \frac{\delta_2}{1 + \delta_2 k_1} (x_2 - k_1 y_1) \\ \dot{y}_2 &= x_2 - k_2 y_2 - \frac{\delta_1 k_2}{1 + \delta_1 k_2} (x_1 - k_2 y_2)\end{aligned}\tag{4}$$

If one adds one more connection between v_1 - v_2 and/or i_1 - i_2 terminals, it is not possible to derive a first-order simultaneous differential equation anymore.

We develop a nonlinear resistor $g(v)$ by using an FET and an inverter. Ref. [Ueta *et al.*, 2004] describes how to realize it. From physical measurement of $g(v)$, we can directly determine parameter values $a = 6.89 \times 10^{-3}$ and $b = 0.3523$. We fix parameters as $L = 10$ [mH], $C = 0.022$ [μ F]. Then the natural frequency of the LC tank is $Z_0 = \sqrt{L/C} = 674.2$ [Ω].

3 Symmetry

This equation has a symmetry in the state space such that

$$\begin{aligned}P : \mathbf{R}^4 &\rightarrow \mathbf{R}^4 \\ (x_1, y_1, x_2, y_2) &\mapsto (-x_1, -y_1, -x_2, -y_2).\end{aligned}\tag{5}$$

This fact directly affects the structure of the state space, namely, if there exists a periodic solution $\varphi(t) \in \mathbf{R}^4$, then $-\varphi(t)$ also forms a periodic solution. Besides the pitchfork bifurcation is possibly caused by this symmetrical property.

There also exist a symmetry in the parameter space:

$$(k_1, k_2, \delta_1, \delta_2) \rightarrow (k_2, k_1, \delta_2, \delta_1)\tag{6}$$

To solve bifurcation problem for attractors in Eq. (4), we use Newton's method with Poincaré mapping. The shooting algorithm like the continuation [Kawakami, 1984] with Newton's method, and its improved algorithm [Ueta *et al.*, 1997] are used for calculation of bifurcation sets in the analysis.

4 Coupling of Identical Oscillators

We firstly analyze the coupled identical oscillators with $k_1 = k_2 = 0.75$. At this parameter values, an individual oscillator exhibits the hard oscillation.

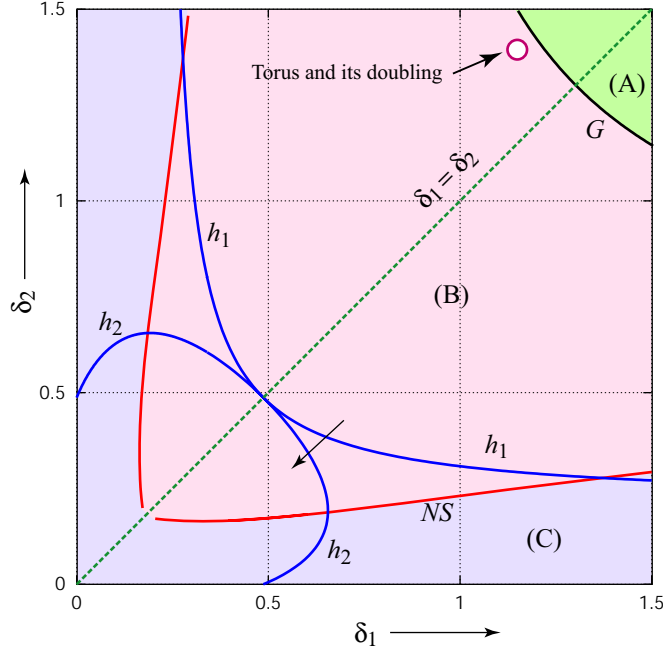


Figure 2: Bifurcation diagram of Eq. (4). $k_1 = k_2 = 0.75$.

Figure 2 shows a bifurcation diagram in δ_1 - δ_2 plane. In the whole parameter region, there consistently exists the three-dimensionally unstable origin. There also exist equilibria $C^\pm = (\pm a, \pm b, \pm a, \pm b)$, a and b are constants. They are stable in area (A). Hopf bifurcation h_1 and h_2 are occurred for C^\pm . By changing parameters along the arrow in the Fig. 2, h_1 , C^\pm become two-dimensionally unstable saddles, and h_2 make this saddle completely unstable. h_1 is related to generation of the in-phase synchronized solution, and h_2 is anti-phase. However, these Hopf bifurcations do not affect extinction of limit cycles.

Bifurcations of limit cycles are governed by the tangent bifurcation G and Neimark-Sacker bifurcation NS in this figure. The anti-phase synchronized solution is disappeared by G as the parameter changes from area (B) to (A), conversely, the in-phase synchronized solution is disappeared by NS as the parameter changes from area (B) to (C). Thus we can split the diagram into three regions:

- In area (A), only a stable anti-phase synchronized solution exists.
- In area (B), both stable in-phase and stable anti-phase synchronized solutions coexist.
- In area (C), only a stable in-phase synchronized solutions exists.

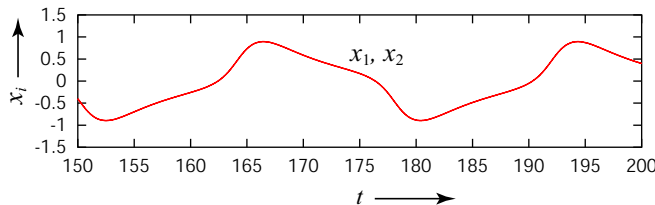
Of course, In area (A) and upper portion of (B) sectioned by h_1 , there also coexist two sinks C^\pm .

If one chooses $\delta_1 = \delta_2 = \delta$ (on the dashed line in the figure), both oscillators become identical. Under this condition, according to parameter values in area (B), we can observe completely synchronized in-phase and anti-phase periodic solutions. Figure 3 (a) shows in-phase and (b) shows anti-phase synchronized solutions, and their appearance depends on the initial value. Notice that these two synchronized solutions contain different base frequencies. We can summarize the following:

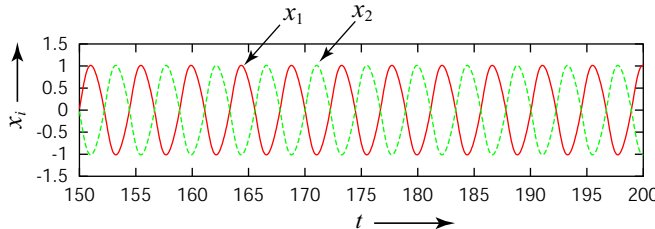
These results follows Papy's, but they mention the case whose k_1 and k_2 are small.

Table 1: Classification of synchronization modes.

| δ | area | mode |
|-------------------------|------|-------------------------|
| small (weak coupling) | (C) | anti-phase |
| medium | (B) | in-phase and anti-phase |
| large (strong coupling) | (A) | in-phase |



(a)



(b)

Figure 3: Time response of x_1 and x_2 , $k_1 = k_2 = 0.75$, $\delta_1 = \delta_2 = 1.0$. (a) completely in-phase synchronization, (b) completely anti-phase synchronization.

5 Torus and its breakdown

Suppose $k_1 = k_2 = 0.75$. Around $1.0 < \delta_1 < 1.4$, $1.0 < \delta_2 < 1.4$ located at area (B) in Fig. 2, there is a stable torus shown in Fig. 4 and Fig. 5 (a). It has been never reported a discovery of a stable torus for coupled identical oscillators because usually tori are unstable (a saddle or repeller type) for identical coupled oscillators. In this system, stable torus, both stable in-phase and anti-phase solutions are coexisted in area (B). Although the generation mechanism of this torus is not clarified yet, we surmise that it is appeared by the trans-critical Neimark-Sacker bifurcation.

As δ_1 increases, the torus is sometimes trapped into periodic solution. However, in some parameter range, the torus meets a bifurcation which looks like the swollen type bifurcation [Sekikawa *et al.*, 2001], see Fig. 5(b). It is very difficult to distinguish whether the torus get doubling or not (Fig. 5(c)). The number of the ‘swollen’ part on the torus is three, and the slightly different δ_1 for this figure, we can observe a stable period-3 orbit.

Note that the swollen bifurcation is occurred after the torus doubling in [Sekikawa *et al.*, 2001]. This snapshots also suggest us a possibility that the swollen bifurcation is one of the degenerated shape of normal torus doubling. By further increment of δ_1 , the doubled torus is distorted via several frequency lockings. The successive torus doubling confirmed in [Sekikawa *et al.*, 2001] cannot be observed before appearance of a chaotic attractor.

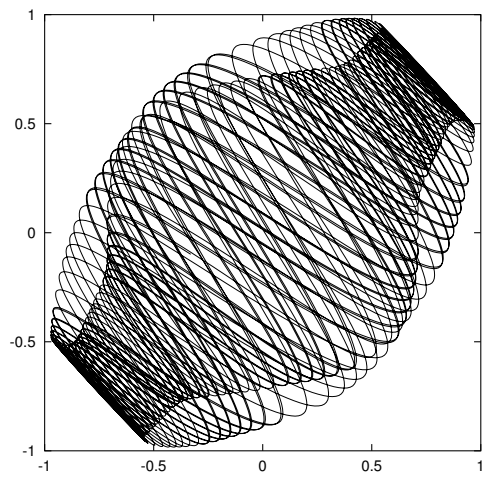


Figure 4: A projection of a torus in y_1 - y_2 plane. $k_1 = k_2 = 0.75$, $\delta_2 = 1.2$.

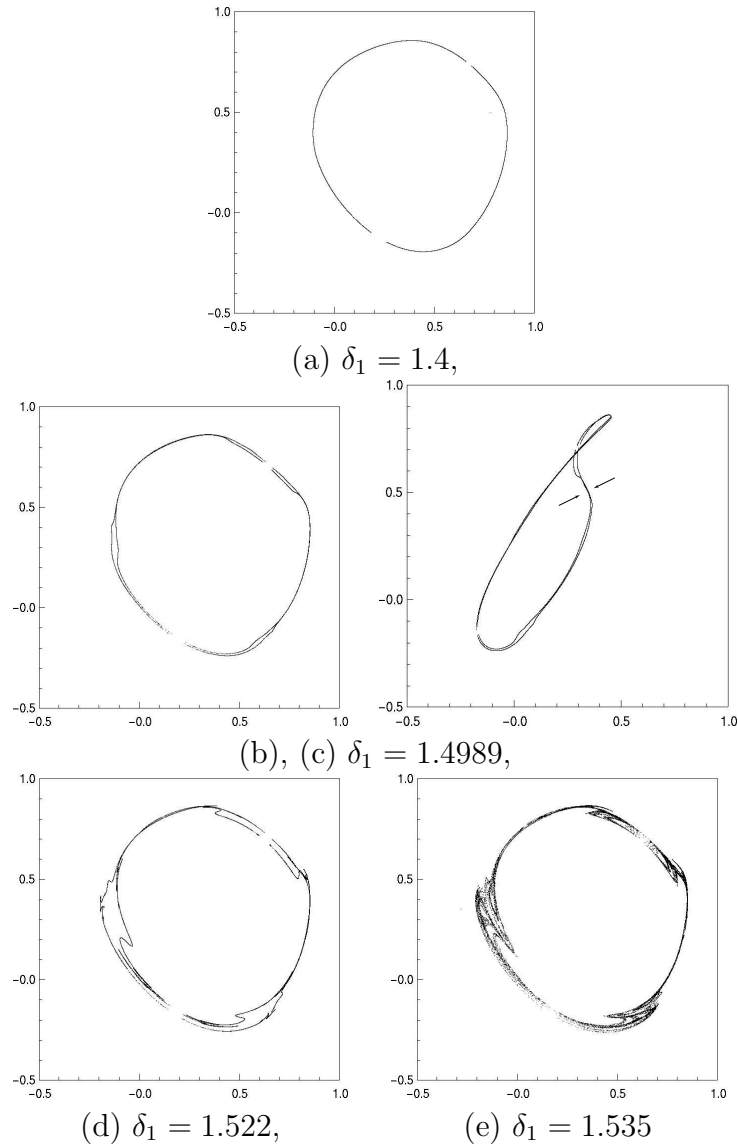


Figure 5: The Poincaré mapping in y_1 - y_2 plane. $k_1 = k_2 = 0.75$, $\delta_2 = 1.2$. The section is $x_0 = 0.9$, (a): Torus (b), (c): Torus doubling, (d): Folding of the invariant closed curve, (e): Chaos.

6 Asymmetrical case

If we choose different values for k_1 and k_2 , basically tori are dominant behavior for weak coupling. Chaos attractors via torus breakdown can be observed in wide range of small values of δ_1 and δ_2 . Since some special cases, such as $\delta_i = 0$, i is 1 or 2, the system is reduced to an asymmetrically coupled BVP system [Ueta & Kawakami, 2003], we easily have period-doubling cascade of limit cycles by selecting parameters. In this way, if we fix $\delta_1 = 0.337$ and $\delta_2 = 2.696$, we can trace period-doubling bifurcation curve in k_1 - k_2 plane, see Fig. 6.

There exist two sinks C^\pm in the area surrounded by h . Pf is the pitchfork bifurcation of the symmetrical limit cycle holding Eq. (5), then the area sectioned by G , Pf and h specifies a region in which the symmetrical limit cycle exists. While asymmetrical periodic solutions after touching the pitchfork bifurcation will meet the period-doubling bifurcation set I . By parameter changing along the arrow, period-doubling cascade and chaos attractors are obtained, see Fig. 7. We confirm same dynamical behavior in an electrical circuitry realizing Eq. (1), see Fig. 8.

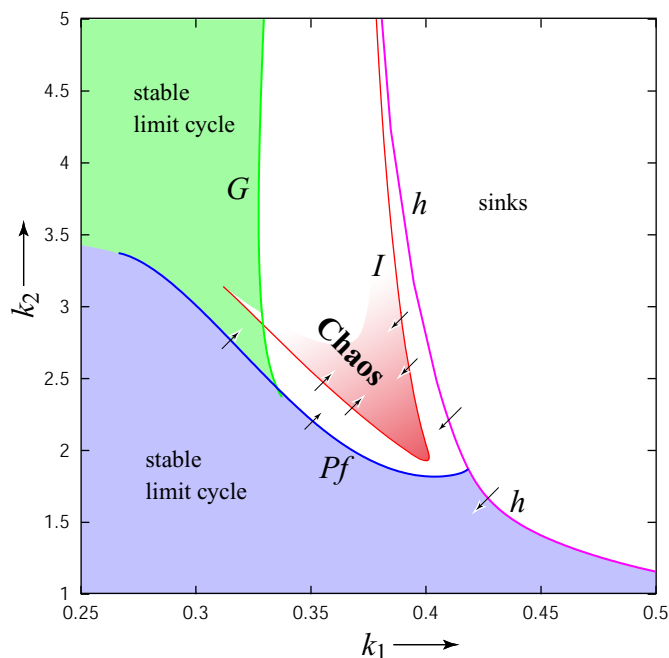


Figure 6: Bifurcation diagram of Eq. (4). $\delta_1 = 0.377$, $\delta_2 = 2.696$.

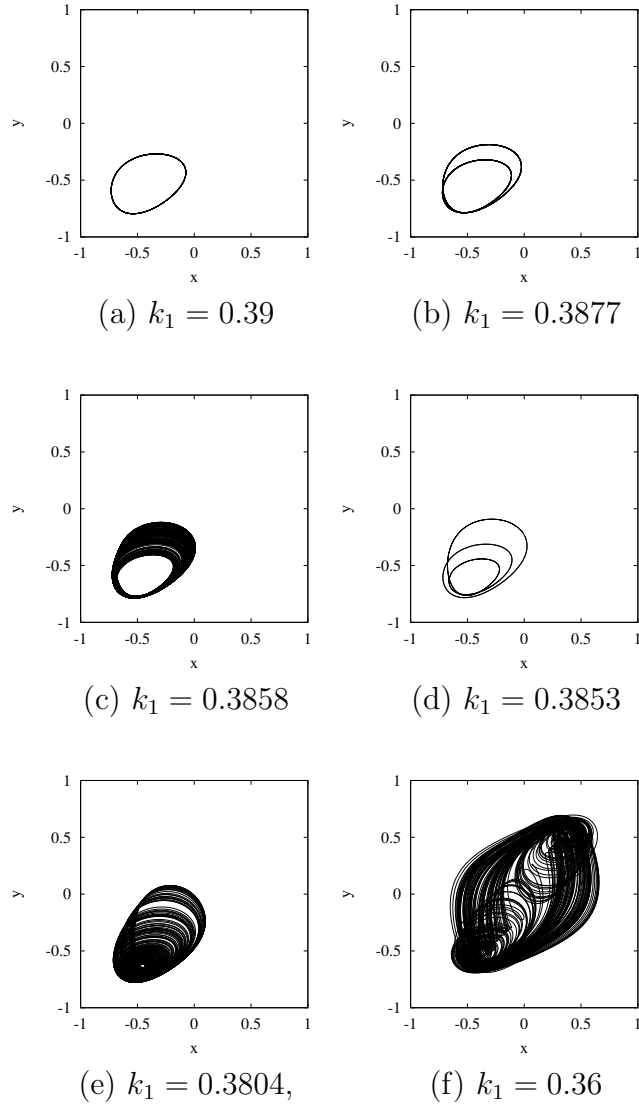


Figure 7: Computer simulations. $k_2 = 2.96$, $\delta_1 = 0.337$, $\delta_2 = 2.696$.

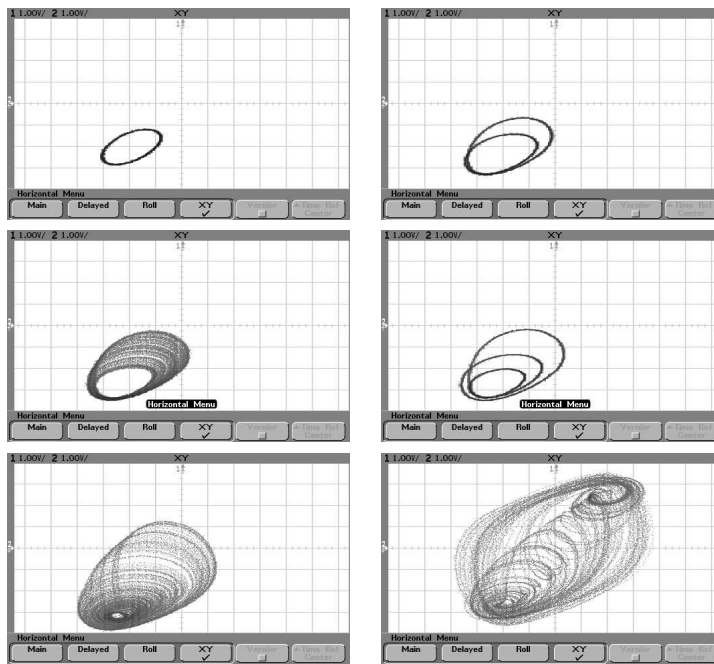


Figure 8: Laboratory experiments corresponding to Fig. 7. $r_2 = 2000[\Omega]$, $G_1 = 1/2000[\mathcal{U}]$, $G_2 = 1/250[\mathcal{U}]$. r_2 is ranged from 216–500 $[\Omega]$.

7 Conclusions

We investigate a cross-coupled BVP oscillators with bifurcation theory. We show bifurcation diagrams for the identical coupled and asymmetrical cases. Torus and its break down is confirmed in the identical coupled oscillators. Period-doubling cascade and chaos attractors are observed in both numerically and experimentally.

References

- [Kawakami, 1984] Kawakami, H., “Bifurcation of Periodic Responses in Forced Dynamic Nonlinear Circuits,” *IEEE Trans. Circuits and Systems*, **CAS-31**, 246–260.
- [Kitajima *et al.*, 1998] H. Kitajima, Y. Katsuta & Kawakami, H., “Bifurcations of periodic solutions in a coupled oscillator with voltage ports,” *IEICE Trans. Fund.* **E81-A**, No.3, 476–482, 1998.
- [Papy & Kawakami, 1995] Papy O. & Kawakami, H., “Symmetrical Properties and Bifurcations of the Periodic Solutions for a Hybridly Coupled Oscillator,” *IEICE Trans. Fund.* **E78-A**, 12, 1816–1821.
- [Papy & Kawakami, 1996] Papy O. & Kawakami, H., “Symmetry Breaking and Recovering in a System of n Hybridly Coupled Oscillators,” *IEICE Trans. Fund.* **E79-A**, 10, 1581–1586.
- [Sekikawa *et al.*, 2001] M. Sekikawa, T. Miyoshi, & N. Inaba. “Successive Torus Doubling,” *IEEE Trans. Circuits and Systems-I*, **CAS-I-48**, 1, 28–34.
- [Ueta *et al.*, 1997] Ueta, T., Tsueike, M., Katsuta, Y., & Kawakami, H., “Computation of bifurcation parameter values for limit cycles,” *IEICE Trans. Fund.* **E80-A**, 1725–1728.
- [Ueta & Kawakami, 2003] Ueta, T. & Kawakami, H., “Bifurcation in asymmetrically coupled BVP oscillators,” *Int. J. of Bifurcation and Chaos*, **13**, 1319–1327.
- [Ueta *et al.*, 2004] Ueta, T., Miyazaki, H., Kousaka, T. & Kawakami, H., “Bifurcation and chaos in coupled BVP oscillators,” *Int. J. Bifurcation and Chaos*, **14**, 1305–1324.